processes

MDPI

Article

A Refractive Index- and Density-Matched Liquid–Liquid System Developed Using a Novel Design of Experiments

Jianxin Tang, Chenfeng Wang, Fei Liu, Xiaoxia Yang and Rijie Wang *

School of Chemical Engineering and Technology, Tianjin University, Tianjin 300350, China; tangjianxin@tju.edu.cn (J.T.); chenfeng_wang@tju.edu.cn (C.W.); 15022364970@163.com (F.L.); xxy@tju.edu.cn (X.Y.)

* Correspondence: rjwang@tju.edu.cn

Abstract: Refractive index and density matching are essential for optical measurements of neutrally buoyant liquid–liquid flows. In this study, we proposed a design of experiments (DoE) to develop refractive index and density matching systems, including objective setting, candidates screening, sampling and fitting, and a detailed matching process. Candidates screening criteria based on the density and refractive index ranges of the aqueous and organic phases were used. Using the DoE, we proposed a system with a ternary aqueous phase potassium thiocyanate (KSCN)/ammonium thiocyanate (NH_4SCN) solution and m-dichlorobenzene/tripropionin solution as the organic phase to achieve the tuning of the RI and density simultaneously. Empirical correlations of the refractive index and density with respect to the concentration and temperature for the three mixtures were obtained by combining Latin hypercube sampling with binary polynomial fitting. Correlations were validated with existing data in the literature and were found to align with deviations as low as 4×10^{-4} for the refractive index and 2×10^{-3} g · cm^{-3} for the density. Using the correlations, the refractive indices for the ternary aqueous phase, the binary organic phase, and the device materials were matched to be equal. Density matching was performed for the liquid–liquid phases as well. Refractive index- and density-matched recipes could be obtained for a wide range of temperatures (15–65 °C) and device materials (PMMA, borosilicate glass, quartz, and silica gel). These recipes provide options for the optical measurement of a liquid–liquid system required to neutralize buoyancy.

Keywords: neutrally buoyant; optical diagnosis; design of experiments; refractive index and density matching; Latin hypercube sampling

Citation: Tang, J.; Wang, C.; Liu, F.; Yang, X.; Wang, R. A Refractive Index- and Density-Matched Liquid–Liquid System Developed Using a Novel Design of Experiments. *Processes* **2023**, *11*, 1922. https://doi.org/10.3390/pr11071922

Received: 8 June 2023
Revised: 22 June 2023
Accepted: 23 June 2023
Published: 26 June 2023

1. Introduction

Neutrally buoyant liquid–liquid flows are widely studied experimentally in droplet formation [1], jet flow [2], and centrifugal extraction [3]. To meet the requirements of neutralizing buoyancy in these applications, density matching is usually necessary to eliminate the density differences between fluid pairs. To examine the local hydrodynamic behavior of the liquid–liquid multiphase flows, laser-induced fluorescence (LIF), laser Doppler velocimetry (LDV), and particle image/tracking velocimetry (PIV/PTV) are widely used as standard tools for flow characterization. These advanced non-invasive, spatiotemporally resolved optical techniques have become standard tools for flow characterization. However, the collection of reliable quantitative data has been dependent on developing related systems for detection or imaging, including lasers, cameras, and photodetectors. Indeed, all these inspection techniques require through-lighting and image acquisition systems. Therefore, two main problems affect the implementation and accuracy when these tools are used in the study of liquid–liquid flows with complex structures. First, optical distortions caused by the reflection and refraction of light when passing through device materials and fluids with different refractive indices (RIs). Second, optical distortions are generated by the refraction of light passing through the flow domain with different RI

fluids. When the RI difference is about 1%, the relative random errors of velocity are as large as 2000% [4]. However, matched density and matched RI are usually not available simultaneously between pure materials. Therefore, it is necessary to develop an RI- and density-matched system consisting of an aqueous phase solution and an organic phase solution. Importantly, to the best of our knowledge, no article to date has been published about such a system.

To summarize, fluid pairs that can be used for optical measurements of neutrally buoyant two-phase flow need to meet the following criteria:

- The RI of the immiscible fluid pairs and device materials need to match.
- The densities of the fluid pairs also need to match.

Previously, numerous relevant experiments reported in the literature were performed with RI-matched liquid–liquid systems. Auger et al. [5] used a two-phase refractive index-matching system with an aqueous glycerol solution with n-heptane to simultaneously measure the velocity and concentration fields of the liquid–liquid system in a simple device with a square structure and surface with no curvature. Morgan et al. [6] used a square test section for horizontal liquid–liquid flow applications. In this work, the RI value of Exxsol D80 was 1.444, which was matched with an 81.7 wt% glycerol solution. Since both studies used a square test section, the RI of the observational solid was not considered. Wright et al. [7] provided a detailed review of refractive index-matching techniques used in liquid–liquid flow studies. They summarized 13 RI-matched liquid–liquid fluid pairs with close RIs based on the study from Smedley and Coles [8]. However, all of the liquid pairs involved single-component liquids and fine tuning of the refractive indices was not possible. This problem can be solved by mixing a third component for both phases. Helmers et al. [9] proposed a method of matching the refractive index using two immiscible binary mixtures to enhance the flexibility of the whole system. Still, some researchers proposed refractive-matching systems for liquid–liquid studies [10–13]. Although there are many RI-matched systems available for liquid–liquid studies, the refractive index of these matching systems is usually different from those of an observational solid. RI-matched liquid–liquid–solid systems are rare and only a few studies have proposed such systems. Burdett et al. [14] matched the refractive indices of silicone rubber (RI = 1.422) with two immiscible fluids. The aqueous phase was a solution of 67.9 wt% glycerol, while the organic phase was methylcyclohexane. Stöhr et al. [15] matched the RI of quartz (RI = 1.458) with two immiscible fluid combinations. The first immiscible fluid was a mixture of silicone oils, consisting of 98 wt% Dow Corning 556 fluid and 2 wt% Dow Corning 200 fluid. The second fluid was an aqueous solution of 58 wt% zinc chloride ($ZnCl_2$). It is surprising that there are no refractive index-matching techniques available for a wider range of solid materials, particularly for commonly used materials, such as PMMA (RI = 1.489) and borosilicate glass (RI = 1.474).

Given that the refractive index is usually the only property considered in the reported systems and other properties tend to be discrepant, the reported physical parameters of RI-matched systems showed a significant density difference between the two phases of the fluid pairs. Density matching for RI-matched fluids is not often taken into account in the diversity and complexity of liquid–liquid matching systems.

Density matching was considered in several solid particle suspension studies. Baily and Yoda [16] proposed a refractive index- and density-matched system for suspension in which polymethyl methacrylate (PMMA) was suspended in a ternary aqueous phase consisting of water, glycerol, and ammonium thiocyanate. They gave an empirical correlation equation for the refractive index expressed in terms of the PMMA particle concentration, chemical composition, and temperature. Wiederseiner et al. [17] reviewed refractive index and density matching in solid particle suspensions and performed optical diagnosis experiments. Nevertheless, density-matched systems have rarely been proposed in the study of liquid–liquid flow. The matching procedure in liquid–liquid systems is more complex than solid–liquid systems because both phases' properties need to be tuned and matched

in liquid–liquid systems. Moreover, a fluid pair's RI needs to be matched to the transparent device material's RI.

For RI matching and density matching, it is important to know the RI and density dependency with composition and temperature. Note that the effect of temperature on the refractive index and density is significant. The problem reduces to determining the relationship between an independent variable (concentration, temperature) and a dependent variable (refractive index, density), i.e., $(RI,\ \rho) = f(c,\ T)$. By using a controlled variable method, the relationships between $(c,\ T)$ and $(RI,\ \rho)$ can be fitted separately. This process requires a huge number of experiments [18] and it is difficult to ensure that the values of the controlled variables are invariant between design points. A stratified random sampling was introduced to counteract such negative effects and included proposing a novel design of experiments (DoE) by coupling Latin hypercube sampling (LHS) with binary polynomial fitting (BPF) and validating the obtained correlations against published data.

To achieve refractive index and density matching with a wider range of applications (temperature range of 15–65 °C, RI range of 1.452–1.489), we proposed a systematic procedure for a RI- and density-matched system that can be used for the optical diagnosis of neutrally buoyant liquid–liquid flows. After a short description of the procedure, the detailed matching process is presented step by step. Two aqueous thiocyanate solutions and an organic binary mixture were selected as candidates. Correlations for refractive index and density were obtained using LHS-BPF. Then, recipes and matching methods for four different transparent materials at different temperatures were created. This procedure is also suitable for developing a matching system for any physical property matching system for liquid–liquid or solid–liquid systems to be studied.

2. Methodology

2.1. Design of Experiments

The DoE described in this paper is shown in Figure 1 and contained four steps, objective setting, candidates screening, sampling and results fitting, and properties matching. The content within the dashed box represents the target property. The two parts connected to the left and right represent the selection of aqueous and organic phases as candidate solutions. This was followed by the data extraction and fitting process of LHS-BPF. Finally, the target recipes of the required solutions were obtained through a matching process.

(1) Objective setting

In addition to determining the refractive index of the solid material, it is essential to identify the properties that require matching. In this study, we planned to develop an RI- and density-matched system consisting of an aqueous phase solution and an organic phase solution, where the RIs of the fluid pairs are matched to PMMA (RI = 1.489), borosilicate glass (RI = 1.474), quartz (RI = 1.458), and silica gel (RI = 1.452).

(2) Candidates screening

The commonly used refractive index matching choices for the aqueous and organic phases are summarized in Tables 1 and 2, respectively. The aqueous phase was designated as a three-component phase to ensure flexibility in the matching process. The organic phase required the selection of two mutually soluble hydrophobic organics with both organic densities between the upper and lower limits of the density of the salt solution.

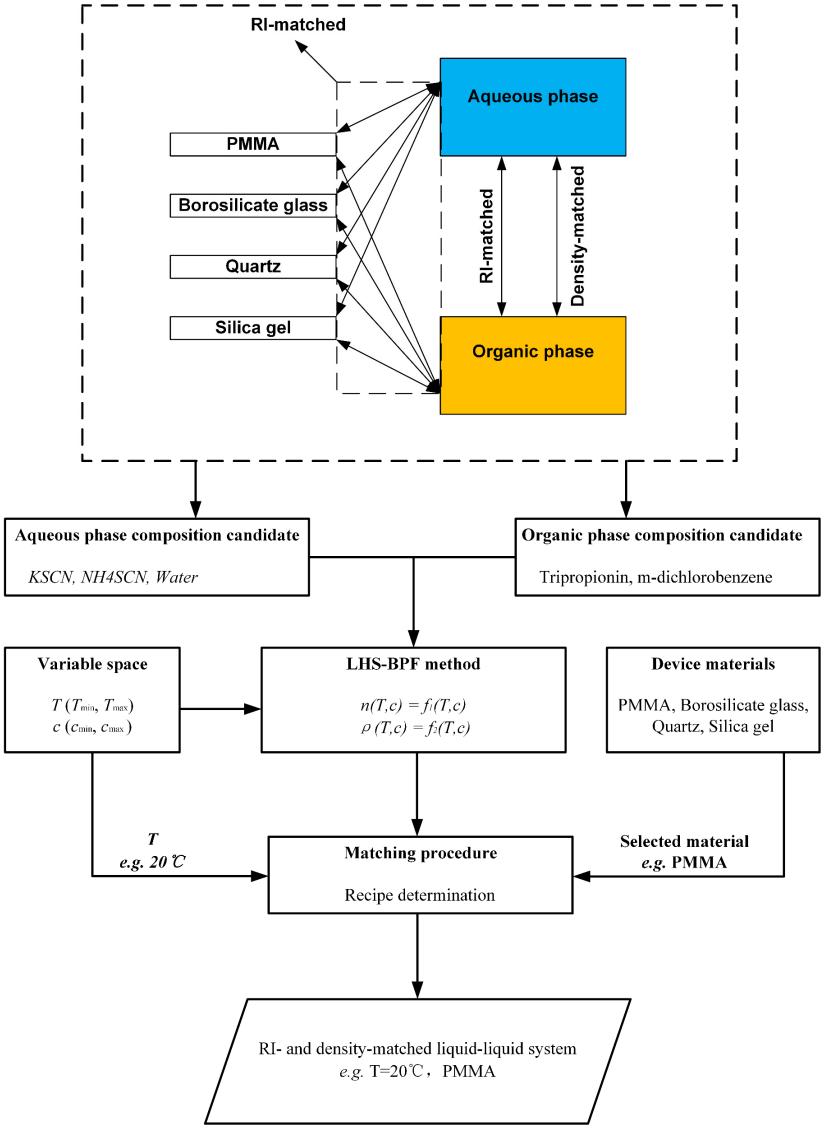

Figure 1. Flow chart of the matching procedure.

Table 1. Common refractive index matching aqueous solutions.

Aqueous Candidates	Range of RI	Range of Density, g/cm^3	Reference
Glycerol (C_3H_8O3)	1.330–1.474	0.998–1.231	Takamura et al. [19]
Potassium thiocyanate (KSCN)	1.330–1.490	0.998–1.414	Jane et al. [20]
Sodium salicylate ($C_7H_5NaO_3$)	1.330–1.490	0.998–1.031	Prasad et al. [21]
Sodium iodide (NaI)	1.330–1.499	0.998–1.283	Bai et al. [22]
Ammonium thiocyanate (NH_4SCN)	1.330–1.503	0.998–1.149	Borrero-Echeverry et al. [23]

Table 2. Common refractive index matching organic liquids.

Organic Candidates	Range of RI	Range of Density, g/cm^3	Reference
Heptane (C_7H_{16})	1.395	0.684	Hibberd et al. [24]
Chloroform ($CHCl_3$)	1.441	1.472	Bhatia et al. [25]
Dow Corning 556	1.460	0.980	Goharzadeh et al. [26]
Xylene (C_8H_{10})	1.493	0.860	Richards et al. [27]
Methyl salicylate ($C_8H_8O_3$)	1.526	1.180	Nguyen et al. [28]
Chloronaphthalene ($C_{10}H_7Cl$)	1.631	1.119	Koh et al. [29]

In this study, the aqueous phase was designated as a three-component phase to provide flexibility in the matching process. The selection of the organic phase required the selection of two mutually soluble non-hydrophilic organics within the density range of the salt solution. Two aqueous thiocyanate solutions with low toxicity and low money cost were selected as candidate aqueous phases, namely, potassium thiocyanate (KSCN) and ammonium thiocyanate (NH_4SCN). NH_4SCN was found to be an ideal refractive index matching medium by several studies [23,30,31]. NH_4SCN was chosen as the target component of the aqueous phase. KSCN is the RI and density adjustment component. Since the two salts have the same anion and similar properties, they provide more flexible and controllable refractive index- and density-matching properties while also ensuring the stability of the aqueous phase. The organics that were reported in the literature that can be used for refractive index matching are all difficult to achieve a compromise between refractive index and density. To this end, a binary organic mixture selection consisting of tripropionin and m-dichlorobenzene was first proposed for RI matching after a simplified calculation. The physical property range of the three solutions used in this study at 20 °C is shown in Figure 2.

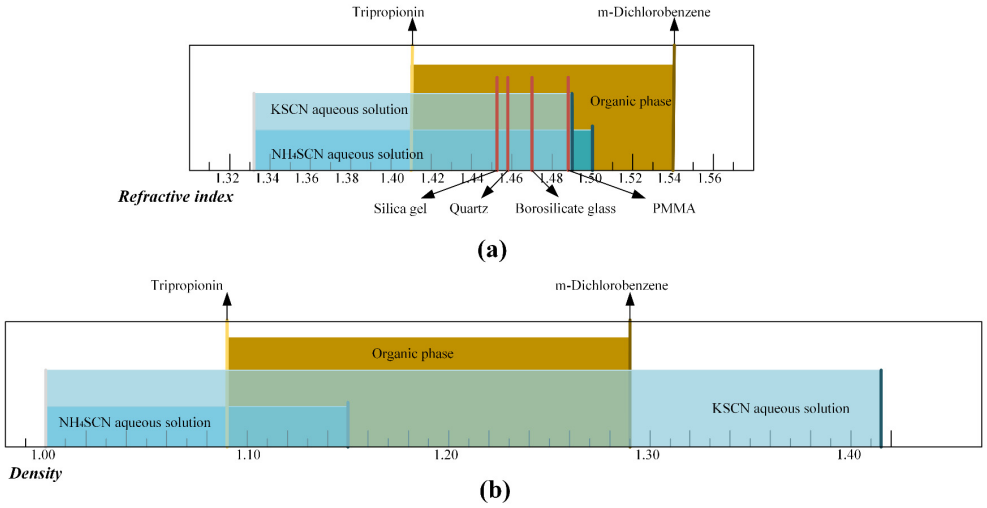

Figure 2. The RI (**a**) and density (**b**) ranges of three fluid pairs at 20 °C.

Figure 2 illustrates the criteria for candidates selecting for the aqueous and organic phases. To achieve a complete refractive index match, the refractive index ranges of both aqueous and organic phase solutions must cover the refractive index ranges of the four different types of solid materials, with overlapping parts. Regarding density, it is necessary to ensure that the density range of the two aqueous phase solutions intersects with the density range of the organic phase. Additionally, the upper limit of the density of one aqueous phase should be higher than the upper limit of the organic phase, while the other aqueous phase should not exceed the upper limit of the organic phase.

(3) Latin hypercube sampling and results fitting

Latin hypercube sampling (LHS) was proposed by McKay et al. [32] and has been used in fluid flow studies [33]. LHS requires that the system being sampled has an invariant underlying logic, and it just needs a few levels to achieve the same goal as a controlled variable method. Since no level appears twice, the total number of experiments is reduced significantly. In this study, every mixed solution is a system with an invariant underlying logic. Temperature T (°C) and concentration c (given by weight percentage) were selected as variables, and correlations of density and refractive index were able to be fitted using a binary polynomial. Python was used to create a 10-run LHS set. The specific sampling results for three candidate solutions are shown in Figure 3, where the black dotted line is the projection of the sampling point on the independent variable. The temperature range for all three fluid pairs studied was 15–65 °C, the concentration range for NH_4SCN

was 0–0.65, the concentration range for KSCN was 0–0.6, and the concentration range for m-dichlorobenzene of the organic phase was 0–1.

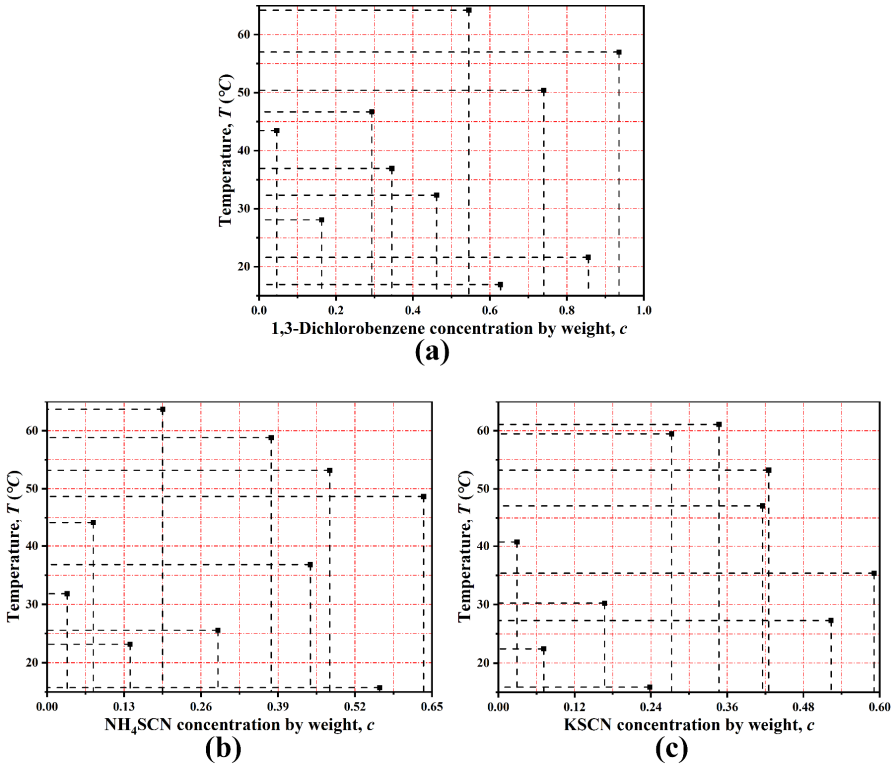

Figure 3. Distribution plot of the Latin hypercube samples.

2.2. Measurement

A METTLER AL204 high-precision electronic balance ensured the accuracy of the mass weighing with an accuracy of 0.0001 g. The temperature-dependent refractive index data were measured using a LICHEN Abbe refractometer at 589 nm with a measurement accuracy of 0.0002. An external, temperature-adjustable circulating water bath controlled the temperature variation in the solution and refractometer to within 0.02 °C. The refractive index of each solution was measured at the design temperature five times and the average value was taken as the measured refractive index for that temperature and composition. The density of each solution at the design temperature was measured using a METTLER DENSITY2GO densimeter with a measurement accuracy of 0.001 g·mL^{-1}.

3. Results and Discussion

Based on the experimental data obtained for each solution, the dependence of the refractive index and density on concentration by weight and temperature for each solution was obtained using binary polynomial fitting. The results of the fitted three-dimensional surfaces are shown in Figure 4a,c,e and Figure 5a,c,e. The relationships between the properties and concentration at different temperatures, which were calculated from the empirical correlations, are shown in Figure 4b,d,f and Figure 5b,d,f. The refractive index and density correlations are described below, and the fitting coefficients are given in Tables 3–6.

Table 3. Coefficients of the empirical correlations for RI.

Fluid Pairs	n_0	$\lambda_{10}\times10^2$	$\lambda_{20}\times10^2$	$\lambda_{01}\times10^4$	$\lambda_{02}\times10^7$	$\lambda_{11}\times10^5$	R^2
Water/NH_4SCN	1.333	23.8	4.121	−1.238	0	−12.6	0.999
Water/KSCN	1.333	17.0	7.067	−1.138	0	−22.5	0.999
1,3-dichlorobenzene/Tripropionin	1.434	9.271	1.869	−4.613	8.201	−1.553	0.999

Table 4. Coefficients of the empirical correlations for the density of the aqueous phase.

Fluid Pairs	φ_{10}	$\varphi_{20}\times10^{2}$	$\varphi_{11}\times10^{4}$	$\varphi_{12}\times10^{5}$	$\varphi_{21}\times10^{3}$	R^2
Water/NH_4SCN	0.2493	0	4.794	2.841	0	0.999
Water/KSCN	0.5459	6.216	−25.1	−2.924	4.899	0.999

Table 5. Coefficients of the empirical correlations for the density of the organic phase.

Fluid Pairs	ρ_T	ϕ_{10}	ϕ_{20}	ϕ_{30}	$\phi_{01}\times10^{4}$	$\phi_{02}\times10^{6}$	$\phi_{11}\times10^{4}$	$\phi_{12}\times10^{5}$	$\phi_{21}\times10^{4}$	R^2
1,3-dichlorobenzene/Tripropionin	1.090	0.2348	−0.1275	0.1119	−6.647	−6.279	−4.838	1.410	−1.935	0.999

Table 6. Coefficients of the empirical correlations for the KSCN solution volume fraction.

Transparent Material	b_0	b_1	$b_2\times10^{3}$	$b_3\times10^{5}$
Quartz	12.80	−0.2374	3.530	2.348
PMMA	26.22	−0.5441	8.140	−0.1184
Borosilicate glass	20.92	−0.4264	6.240	0.9598
Silica gel	9.125	−0.2374	3.530	2.348

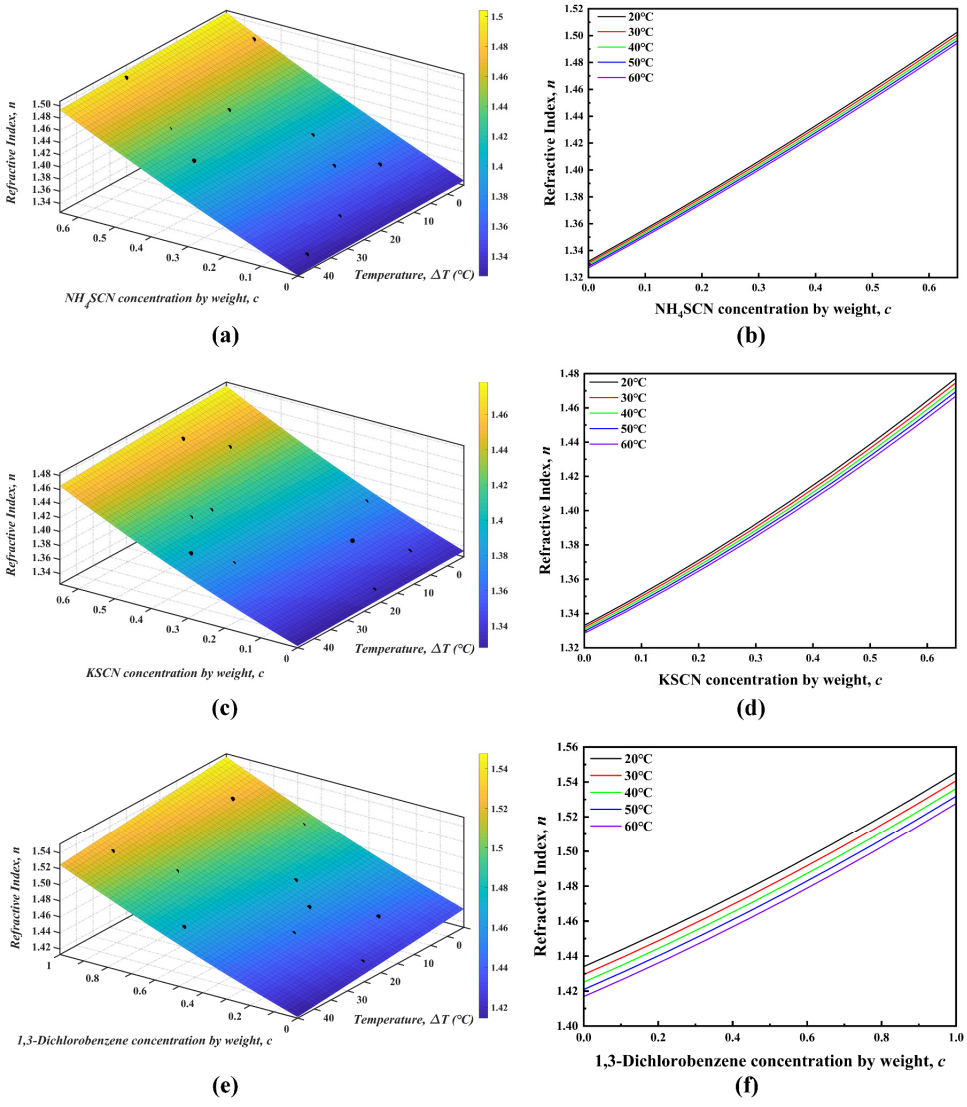

Figure 4. Refractive index fitting result plots: (**a**,**c**,**e**) RI vs. concentration and temperature and (**b**,**d**,**f**) RI vs. concentration at different temperatures.

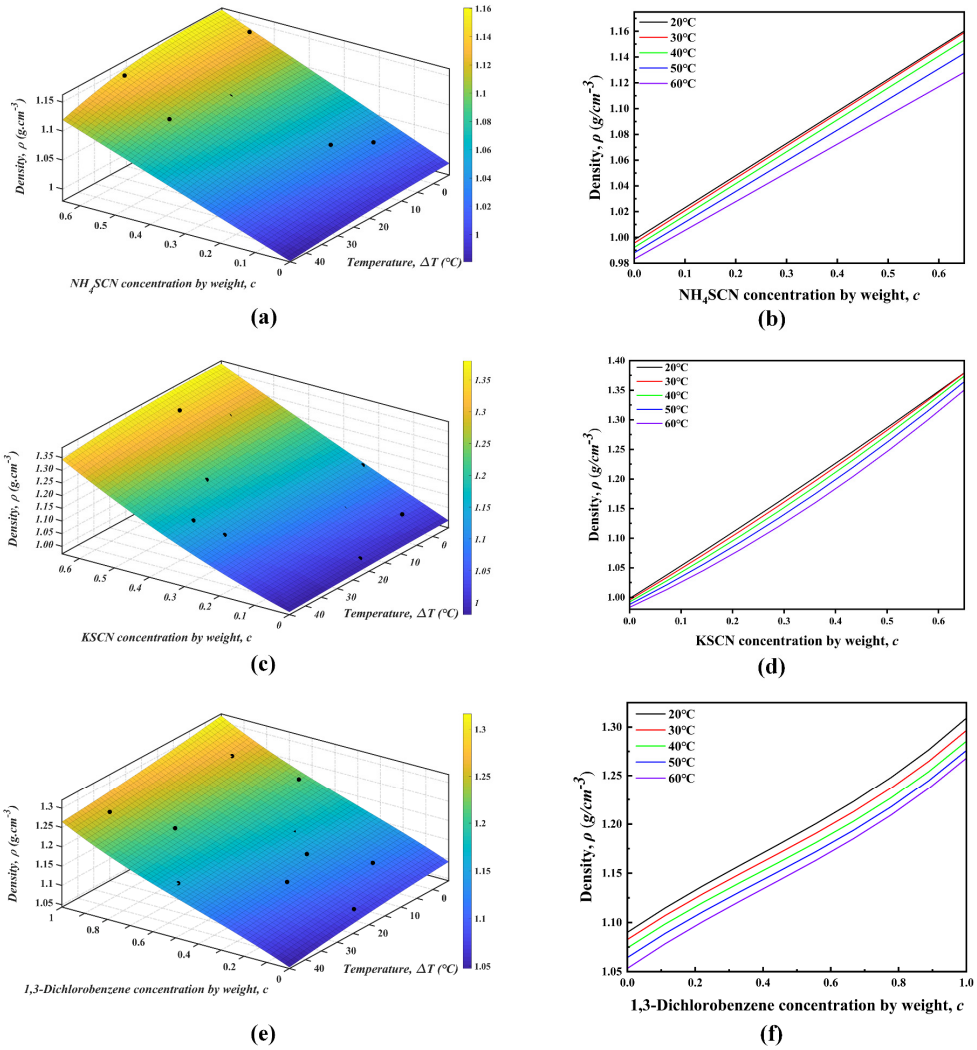

Figure 5. Density fitting result plots: (**a**,**c**,**e**) density vs. concentration and temperature and (**b**,**d**,**f**) density vs. concentration at different temperatures.

3.1. Refractive Index Correlations

The empirical correlations of the refractive index of three fluid pairs in the temperature and concentration ranges mentioned above at a fixed measurement wavelength can all be expressed as Equation (1), where the RI of the two aqueous phase solutions has a quadratic relationship with concentration and a linear relationship to temperature. A second order is used for both concentration and temperature for the organic phase. The linear cross-term represents the coupling between concentration and temperature dependencies.

$$n = n_0 + \lambda_{10}c + \lambda_{20}c^2 + \lambda_{01}\Delta T + \lambda_{02}\Delta T^2 + \lambda_{11}c\Delta T \quad (1)$$

where n is the RI; c is the mass concentration of the target compound in each solution; temperature is given by $\Delta T = T - T_0$, where $T_0 = 20$ °C; and λ_{ij} is the fitting coefficient. The value n_0 represents the RI of water at 20 °C with a value of 1.333 for the aqueous phase or the RI of tripropionin (i.e., m-dichlorobenzene at a mass concentration of 0) at 20 °C with a value of 1.434 for the organic phase. The regression coefficients R^2 were all more than 0.999, indicating that the data fit well.

The high R^2 values not only demonstrated the accuracy of the fitting method utilized in this study but also highlighted the crucial role of Latin hypercube sampling (LHS). The LHS method not only significantly reduced the total number of experiments but also ensured that the sampled data points were more representative in the variable space. As a

result, the association results obtained were strongly correlated. Thus, the combination of LHS and BPF was well-suited for use in physical data correlation applications.

3.2. Density Correlations

The density of an aqueous phase solution can be correlated with the density of pure water versus temperature, superimposed on the term of concentration effect and some series of temperature and the concentration interaction term. The NH_4SCN aqueous solution density and concentration exhibited a linear relationship, while a KSCN aqueous solution showed a second-order relationship. The general formula of the empirical correlation is expressed as Equation (2):

$$\rho_A = \rho_0 + \varphi_{10}c + \varphi_{20}c^2 + \varphi_{11}c\Delta T + \varphi_{12}c\Delta T^2 + \varphi_{21}c^2\Delta T \quad (2)$$

$$\rho_0 = 0.9982 - 2.056 \times 10^{-4}\Delta T - 4.851 \times 10^{-6}\Delta T^2 + 1.588 \times 10^{-8}\Delta T^3 \quad (3)$$

where ρ_0 is the density of pure water at atmospheric pressure versus temperature, as shown in Equation (3). The value 0.9982 [34] represents the density of water at 20 °C.

The density of the organic phase had a cubic relationship with the concentration of m-dichlorobenzene (weight percentage) and a quadratic relationship with temperature, as shown in Equation (4), where ρ_T is the density of tripropionin at 20 °C with a value of 1.090 g·cm^{-3}, which is similar to the results of Smedly et al. [8].

$$\rho_O = \rho_T + \phi_{10}c + \phi_{20}c^2 + \phi_{30}c^3 + \phi_{01}\Delta T + \phi_{02}\Delta T^2 + \phi_{11}c\Delta T + \phi_{21}c^2\Delta T + \phi_{12}c\Delta T^2 \quad (4)$$

3.3. Validation of Fitting Correlations

The validity of the LHS-BPF method was evaluated along with the accuracy of the experimental measurements. First, the empirical correlations obtained using the LHS-BPF method were compared with the data acquired via the controlled variable method. As shown in Figure 6a,b, the difference between the measured and predicted refractive index values of all points at this temperature was less than 4×10^{-4}. Subsequently, correlations were verified using the refractive index and density data published by Agrawal et al. [35]. The results showed that the refractive index difference was lower than 4×10^{-4}, and the difference in the densities was less than 2×10^{-3} g · cm^{-3} in Figure 6c,d. The minimal difference in the above results also showed the effectiveness of the LHS-BPF method proposed in the physical property correlation of hybrid solutions. Furthermore, all the data obtained in this study versus the value calculated using empirical correlations shown in Figure 7 demonstrated the accuracy of the correlations.

3.4. Process for Refractive Index and Density Matching

The empirical correlations for the RIs of the three fluid pairs could determine the composition of the mixture that matches the RIs of the different transparent materials at different temperatures, as shown in Figure 8. The densities of the three mixtures at a certain temperature could be obtained through the density empirical correlations. When the RIs of two phases were matched with transparent materials, the density difference between the NH_4SCN solution and the organic phase at different temperatures is shown in Figure 9. Four commonly used transparent materials were analyzed, and their RIs in descending order were 1.489 (PMMA), 1.474 (borosilicate glass), 1.458 (quartz), and 1.452 (silica gel). As shown in Figure 9, the lowest value of the density difference between the two phases existed along with temperature when matching the same material in the studied temperature range, which followed the polynomial law. When comparing transparent materials, the greater the material's RI, the greater the density difference between aqueous and organic phases was. The density difference between the two phases could be reconciled by introducing a certain amount of RI-matched KSCN aqueous solution into the water phase. The ternary mixture readily achieved the compromise between the refractive index and density.

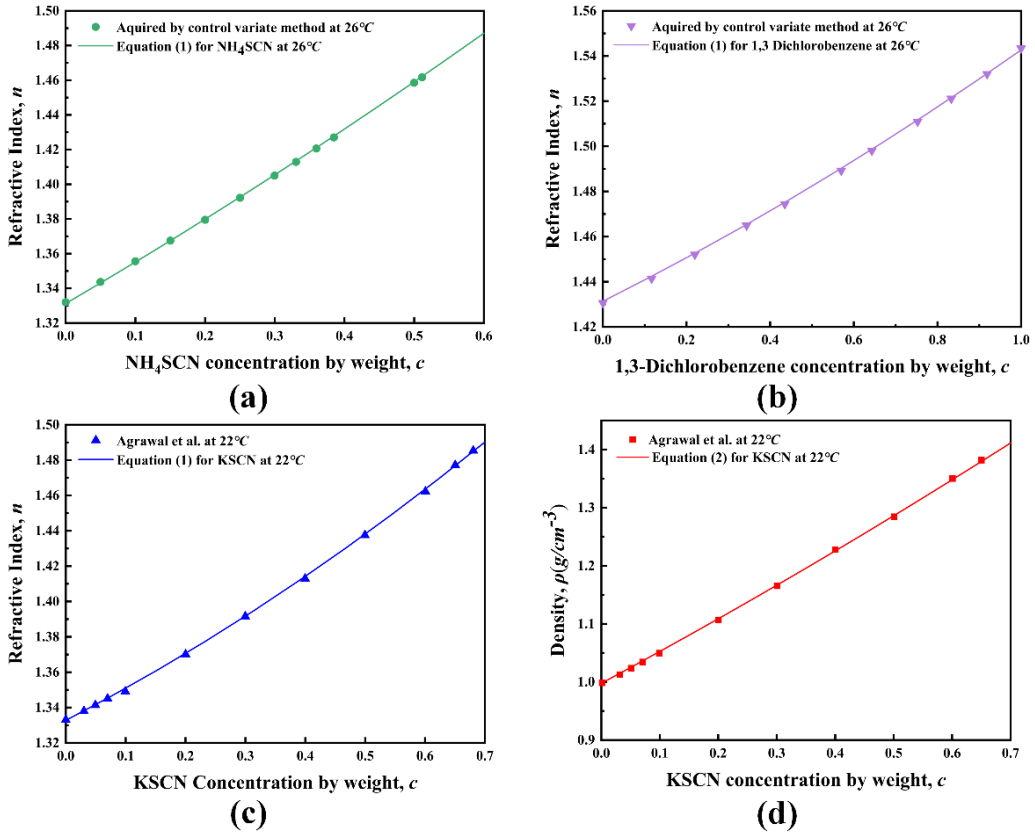

Figure 6. Validation of the fitting correlation plots: comparison with the experimental data acquired via the controlled variate method (**a**,**b**) and the data from Agrawal et al. [35] at 22 °C (**c**,**d**).

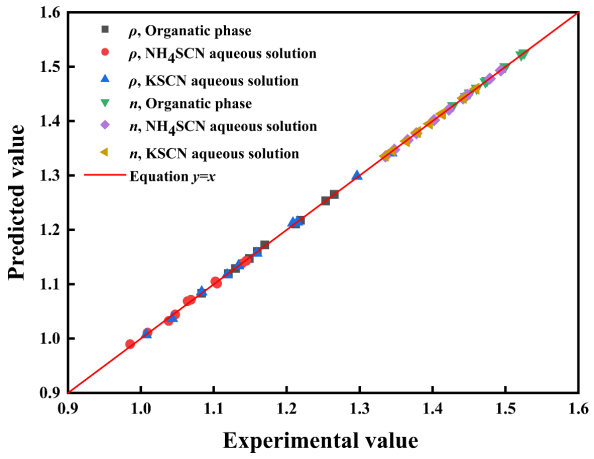

Figure 7. Parity plot of the experimental value and the predicted value for all data.

Usually, the physical properties of ternary mixtures present a ternary triangular relationship. Clement et al. [36] investigated non-linear effects when mixing RI-matched binary solutions. The results showed that the density and RI of the ternary mixed solution follow a linear model. Therefore, the densities of RI-matched NH_4SCN and KSCN aqueous solutions after mixing could be calculated according to Equation (5):

$$\rho_m = \theta\rho_P + (1-\theta)\rho_A \quad (5)$$

where ρ_m is the density of the solution after mixing; ρ_P and ρ_A are the densities of KSCN and NH_4SCN aqueous solutions with matched RI, respectively; and θ is the volume fraction of the KSCN aqueous solution required for mixing. Thus, as shown in Figure 10, we could

obtain the volume fraction of KSCN aqueous solution for different transparent materials at different temperatures. The volume fraction as a function of temperature for transparent material could be expressed as shown in Equation (6). The coefficients for the different transparent materials considered are summarized in Table 6. The recipe of the aqueous solution could be adjusted according to the transparent material of the experimental setup and the experimental temperature.

$$\theta = b_0 + b_1 T + b_2 T^2 + b_3 T^3 \quad (6)$$

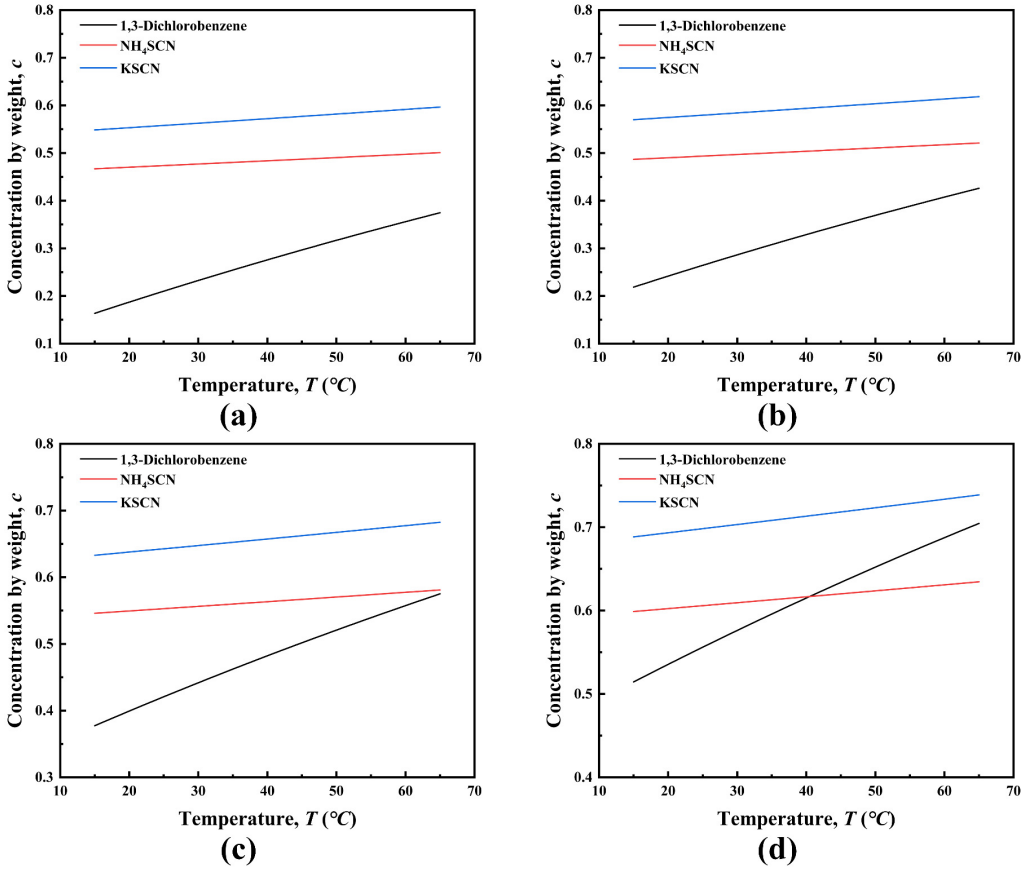

Figure 8. Aqueous and organic phase composition at different temperatures when the refractive index was matched with silica gel (**a**), quartz (**b**), borosilicate glass (**c**), and PMMA (**d**).

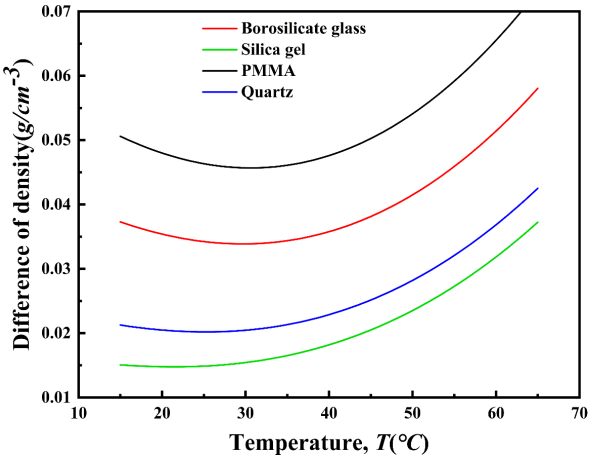

Figure 9. Density difference between the RI-matched organic phase and NH_4SCN solutions at different temperatures with different transparent materials.

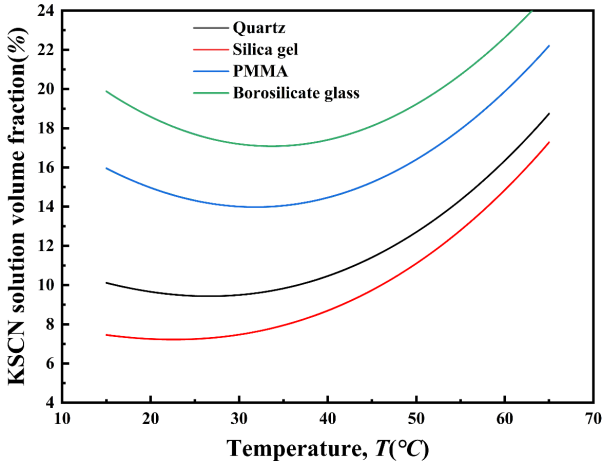

Figure 10. KSCN solution volume fraction in the mixed aqueous solution at different temperatures when the RI was matched with different transparent materials.

The matching process described above allowed for the determination of matching requirements based on the material of the device and the temperature of the experiment. The composition of the three required solutions could be determined separately by using the correlation equations for refractive index and density. The volume ratio of the two aqueous phase solutions could be calculated using Equation (6). Afterward, the aqueous phase solutions are blended based on fixed ratios. The goal was to achieve a liquid–liquid two-phase system with matching refractive indices and densities, where both refractive indices matched those of the device materials. This design of experiments (DoE) covered almost the full range of temperatures and refractive indices required for equipment materials in hydrodynamic experiments. Furthermore, this method is easily replicable in common experimental conditions.

4. Conclusions

This study proposed a novel DoE to develop a RI- and density-matched system for neutrally buoyant two-phase flows. An RI- and density-matched system was successfully obtained with a KSCN/NH_4SCN aqueous solution as the aqueous phase and an m-dichlorobenzene/tripropionin solution as the organic phase. The system can be flexibly tuned for a wide range of experimental temperatures (15–65 °C) and the type of different solid materials (RI = 1.452–1.489). The use of three-component aqueous solutions to reconcile the refractive index and density was shown to be effective.

The method combining Latin hypercube sampling with binary polynomial fitting was used to acquire accurate empirical correlations of refractive index and density with a minimum number of experiments. The generated empirical correlations were validated using the results of previous studies, as the results showed that the refractive index difference was lower than 4×10^{-4}, and the difference in densities was less than 2×10^{-3} g · cm^{-3}. This method of obtaining accurate correlations of physical properties data with limited data points can serve as a reference for other physical properties studies.

The matching procedure and DoE proposed in this study can be applied not only to the development of liquid–liquid systems that match the refractive index and density but also to the more complex matching of multiple properties, such as particle–liquid–liquid–solid systems. This provides new ideas for more diverse property matching requirements and more complex matching processes.

Author Contributions: Conceptualization, J.T.; methodology, C.W.; software, C.W.; validation, J.T. and C.W.; formal analysis, J.T.; data curation, F.L.; writing—original draft preparation, J.T.; writing—review and editing, C.W.; supervision, X.Y.; project administration, R.W. All authors have read and agreed to the published version of the manuscript.

Funding: This research received no funding.

Conflicts of Interest: The authors declare no conflict of interest.

Nomenclature

Symbols	
b	Fitting coefficients in correlations of the KSCN aqueous solution's volume fraction
BPF	Binary polynomial fitting
c	Concentration by weight (weight percentage)
LHS	Latin hypercube sampling
n_i	The symbol for refractive index
n_0	Refractive index of water at 20 °C
R^2	Correlation coefficient squares
RI	Refractive index
T	Temperature, °C
T_0	The initial temperature, 20 °C
ΔT	Temperature difference
Greek symbols	
ρ_i	Density, $g \cdot cm^{-3}$
μ	Viscosity, $mPa \cdot s$
θ	Volume fraction of KSCN aqueous solution required for mixing.
λ_{ij}	Fitting coefficients in correlations of refractive index
φ_{ij}	Fitting coefficients in correlations of aqueous phase's density
ϕ_{ij}	Fitting coefficients in correlations of organic phase's density

References

1. Gao, Y.; Mitra, S.; Wanless, E.J.; Moreno-Atanasio, R.; Evans, G.M. Interaction of a spherical particle with a neutrally buoyant immiscible droplet in salt solution. *Chem. Eng. Sci.* **2017**, *172*, 182–198. [CrossRef]
2. Ryu, Y.; Chang, K.; Mori, N. Dispersion of neutrally buoyant horizontal round jet in wave environment. *J. Hydraul. Eng.* **2005**, *131*, 1088–1097. [CrossRef]
3. Spandan, V.; Lohse, D.; Verzicco, R. Deformation and orientation statistics of neutrally buoyant sub-kolmogorov ellipsoidal droplets in turbulent taylor–couette flow. *J. Fluid Mech.* **2016**, *809*, 480–501. [CrossRef]
4. Li, H.; Fischer, A.; Avila, M.; Xu, D. Measurement error of tracer-based velocimetry in single-phase turbulent flows with inhomogeneous refractive indices. *Exp. Therm. Fluid Sci.* **2022**, *136*, 110681. [CrossRef]
5. Augier, F.; Masbernat, O.; Guiraud, P. Slip velocity and drag law in a liquid-liquid homogeneous dispersed flow. *AICHE J.* **2003**, *49*, 2300–2316. [CrossRef]
6. Morgan, R.G.; Markides, C.N.; Hale, C.P.; Hewitt, G.F. Horizontal liquid–liquid flow characteristics at low superficial velocities using laser-induced fluorescence. *Int. J. Multiph. Flow* **2012**, *43*, 101–117. [CrossRef]
7. Wright, S.F.; Zadrazil, I.; Markides, C.N. A review of solid–fluid selection options for optical-based measurements in single-phase liquid, two-phase liquid–liquid and multiphase solid–liquid flows. *Exp. Fluids* **2017**, *58*, 108. [CrossRef]
8. Smedley, G.; Coles, D. Some transparent immiscible liquid pairs. *J. Colloid Interface Sci.* **1990**, *138*, 42–60. [CrossRef]
9. Helmers, T.; Kemper, P.; Mießner, U.; Thöming, J. Refractive index matching (rim) using double-binary liquid–liquid mixtures. *Exp. Fluids* **2020**, *61*, 64. [CrossRef]
10. Chen, R.C.; Kadambi, J.R. Discrimination between solid and liquid velocities in slurry flow using laser doppler velocimeter. *Powder Technol.* **1995**, *85*, 127–134. [CrossRef]
11. Amini, N.; Hassan, Y.A. An investigation of matched index of refraction technique and its application in optical measurements of fluid flow. *Exp. Fluids* **2012**, *53*, 2011–2020. [CrossRef]
12. Reddy, R.K.; Sathe, M.J.; Joshi, J.B.; Nandakumar, K.; Evans, G.M. Recent developments in experimental (piv) and numerical (dns) investigation of solid–liquid fluidized beds. *Chem. Eng. Sci.* **2013**, *92*, 1–12. [CrossRef]
13. Ghatage, S.V.; Peng, Z.; Sathe, M.J.; Doroodchi, E.; Padhiyar, N.; Moghtaderi, B.; Joshi, J.B.; Evans, G.M. Stability analysis in solid–liquid fluidized beds: Experimental and computational. *Chem. Eng. J.* **2014**, *256*, 169–186. [CrossRef]
14. Burdett, I.D.; Webb, D.R.; Davies, G.A. A new technique for studying dispersion flow, holdup and axial mixing in packed extraction columns. *Chem. Eng. Sci.* **1981**, *36*, 1915–1919. [CrossRef]
15. Stöhr, M.; Roth, K.; Jähne, B. Measurement of 3d pore-scale flow in index-matched porous media. *Exp. Fluids* **2003**, *35*, 159–166. [CrossRef]
16. Bailey, B.C.; Yoda, M. An aqueous low-viscosity density- and refractive index-matched suspension system. *Exp. Fluids* **2003**, *35*, 1–3. [CrossRef]

17. Wiederseiner, S.; Andreini, N.; Epely-Chauvin, G.; Ancey, C. Refractive-index and density matching in concentrated particle suspensions: A review. *Exp. Fluids* **2011**, *50*, 1183–1206. [CrossRef]
18. Han, S.; Du, C.; Jian, X.; Meng, L.; Ren-Jie, X.; Jian, W.; Zhao, H. Density, viscosity, and refractive index of aqueous solutions of sodium lactobionate. *J. Chem. Eng. Data* **2016**, *61*, 731–739. [CrossRef]
19. Takamura, K.; Fischer, H.; Morrow, N.R. Physical properties of aqueous glycerol solutions. *J. Pet. Sci. Eng.* **2012**, *98*, 50–60. [CrossRef]
20. Jan, D.L.; Shapiro, A.H.; Kamm, R.D. Some features of oscillatory flow in a model bifurcation. *J. Appl. Physiol.* **1989**, *67*, 147–159. [CrossRef]
21. Prasad, V.; Brown, K.; Tian, Q. Flow visualization and heat transfer experiments in fluid-superposed packed beds heated from below. *Exp. Therm. Fluid Sci.* **1991**, *4*, 12–24. [CrossRef]
22. Bai, K.; Katz, J. On the refractive index of sodium iodide solutions for index matching in piv. *Exp. Fluids* **2014**, *55*, 1704. [CrossRef]
23. Borrero-Echeverry, D.; Morrison, B.C.A. Aqueous ammonium thiocyanate solutions as refractive index-matching fluids with low density and viscosity. *Exp. Fluids* **2016**, *57*, 123. [CrossRef]
24. Hibberd, D.J.; Mackie, A.R.; Moates, G.K.; Penfold, R.; Watson, A.D.; Barker, G.C. Preparation and characterisation of a novel buoyancy and refractive index matched oil-in-water emulsion. *Colloids Surf. A Physicochem. Eng. Asp.* **2007**, *301*, 453–461. [CrossRef]
25. Bhatia, S.C.; Bhatia, R.; Dubey, G.P. Refractive properties and internal pressures of binary mixtures of octan-1-ol with chloroform, 1,2-dichloroethane and 1,1,2,2-tetrachloroethane at 298.15 and 308.15 k. *J. Mol. Liq.* **2009**, *145*, 88–102. [CrossRef]
26. Goharzadeh, A.; Khalili, A.; Jørgensen, B.B. Transition layer thickness at a fluid-porous interface. *Phys. Fluids* **2005**, *17*, 57102. [CrossRef]
27. Richards, J.R.; Scheele, G.F. Measurement of laminar jet velocity distributions in liquid-liquid systems using flash photolysis. *Chem. Eng. Commun.* **1985**, *36*, 73–92. [CrossRef]
28. Nguyen And, T.T.; Biadillah, Y.; Mongrain, R.; Brunette, A.J.; Tardif, J.; Bertrand, O.F. A method for matching the refractive index and kinematic viscosity of a blood analog for flow visualization in hydraulic cardiovascular models. *J. Biomech. Eng.* **2004**, *126*, 529–535. [CrossRef]
29. Koh, C.J.; Hookham, P.; Leal, L.G. An experimental investigation of concentrated suspension flows in a rectangular channel. *J. Fluid Mech.* **1994**, *266*, 1–32. [CrossRef]
30. Budwig, R.; Elger, D.; Hooper, H.; Slippy, J. Steady flow in abdominal aortic aneurysm models. *J. Biomech. Eng. Trans. ASME* **1993**, *115*, 418–423. [CrossRef]
31. Egelhoff, C.J.; Budwig, R.S.; Elger, D.F.; Khraishi, T.A.; Johansen, K.H. Model studies of the flow in abdominal aortic aneurysms during resting and exercise conditions. *J. Biomech.* **1999**, *32*, 1319–1329. [CrossRef]
32. Mckay, M.D.; Conover, R.J.B.J. A comparison of three methods for selecting values of input variables in the analysis of output from a computer code. *Technometrics* **1979**, *21*, 239–245.
33. Jiang, X.; Xiao, Z.; Jiang, J.; Yang, X.; Wang, R. Effect of element thickness on the pressure drop in the kenics static mixer. *Chem. Eng. J.* **2021**, *424*, 130399. [CrossRef]
34. Wagner, W.; Pruß, A. The iapws formulation 1995 for the thermodynamic properties of ordinary water substance for general and scientific use. *J. Phys. Chem. Ref. Data* **2002**, *31*, 387–535. [CrossRef]
35. Agrawal, Y.K.; Sabbagh, R.; Sanders, S.; Nobes, D.S. Measuring the refractive index, density, viscosity, ph, and surface tension of potassium thiocyanate (kscn) solutions for refractive index matching in flow experiments. *J. Chem. Eng. Data* **2018**, *63*, 1275–1285. [CrossRef]
36. Clément, S.A.; Guillemain, A.; Mccleney, A.B.; Bardet, P.M. Options for refractive index and viscosity matching to study variable density flows. *Exp. Fluids* **2018**, *59*, 32. [CrossRef]